Electronic Supporting Information

Structural tailoring of the NIR-absorption of bis(1,2-dichalcogenolene) Ni/Pt electrochromophores deriving from 1,3-dimethyl-2-chalcogenoxo-imidazoline-4,5-dichalcogenolates

Carlo Deiana, M. Carla Aragoni, Francesco Isaia, Vito Lippolis, Anna Pintus, Alexandra M. Z. Slawin, Derek J. Woollins and Massimiliano Arca*

Materials and Methods.

All the syntheses were carried out under inert atmosphere. The solvents were of reagent grade, and were dried by using standard techniques. Elemental analyses were performed with an EA1108 CHNS-O Fisons Instrument (T = 1000° C). FT-MIR spectra were recorded with a Thermo-Nicolet 5700 spectrometer at room temperature: KBr pellets with a KBr beam-splitter and KBr windows (4000–400 cm^{-1}, resolution 4 cm^{-1}) were used. FT-FIR spectra were recorded on a Bruker IFS55 spectrometer at room temperature, purging the sample cell with a flow of dried air. Polythene pellets with a mylar beam-splitter and polythene windows (500–50 cm^{-1}, resolution 2 cm^{-1}) were used. FT-Raman spectra (resolution of 4 cm^{-1}) were recorded on a Bruker RFS100 FT-Raman spectrometer, fitted with an In-Ga-As detector (room temperature) operating with a Nd-YAG laser (excitation wavelength 1064 nm). Cyclic voltammetry (CV) measurements were recorded at scan rate 0.1 V s^{-1}, using an EG&G Model 273 at 20°C in a Metrohm voltammetric cell, with a combined working and counter Pt electrode and a standard Ag/AgCl (in KCl 3.5 M) reference electrode. Tetrabutylammonium tetrafluoroborate was used as a supporting electrolyte ($5\cdot10^{-2}$ M). Spectrophotometric titrations were recorded by adding increasing amounts of a diiodine CH_2Cl_2 solution ($C = 7.00\cdot10^{-4}$ M) to weighed amounts of the bis(1,2-dichalcogenolene) metal complexes. Absorption spectra were recorded at 298 K in a quartz cell of 10.00 mm optical path with a Thermo Evolution 300 (UV-Vis) and an Agilent Technologies Cary 5000 (UV-Vis-NIR) spectrophotometers. NIR spectra were recorded on CH_2Cl_2, $CHCl_3$, CH_3CN, THF and DMF solutions in the range 800-2000 nm. Depending on the complex, because of low solubility reasons, the absorption maxima value were extrapolated with a linear least squares method on the values recorded on mixed solvents solutions prepared according to different V_{solv}/V_{CH2Cl2} values. Single crystal X-ray diffraction data for compound **9** were collected with the St. Andrews Robotic diffractometer at 93(2) K.[1] The structure was solved by direct methods with SHELXS-97[2] and refined on F^2 by using SHELXL2013 (deposition number CCDC 1484547).[3] Theoretical calculations were performed at Density

Functional Theory (DFT) level[4] with the Gaussian 09 suite of programs[5] on a E4 workstation equipped with four 4-core processors and 16 Gb of RAM (OS: Ubuntu 14.04 Linux) and on a IBM x3755 server with four 12-core processors and 64 Gb of RAM (OS: SUSE Linux Enterprise Server 11 SP3). A preliminary validation of the computational setup was carried out by comparing the metric parameters optimized for complex **1** with those reported for the complexes [Ni(R,R'timdt)$_2$] structurally characterized so far[6,7,8] and the unscaled NIR absorption wavelength calculated at TD-DFT level with the experimental one (995 nm) measured experimentally in CH_2Cl_2 at room temperature. Schäfer, Horn, and Ahlrichs double-ζ plus polarization (pVDZ) all-electron basis sets[9] (BS) were used for C, H, N, S, and Se. The LANL08(f),[10] SBKJC,[11] Stuttgart 1997 RC,[12] CRENBL,[13] LANL2DZ,[14] and LANL2TZ[10] BS's with Relativistic Effective Core Potentials (RECPs)[15,16] were tested for the central metal ion. Basis sets were obtained from Basis Set Exchange and Basis Set EMSL Library.[17] All tests were repeated with three hybrid functionals, namely Becke3LYP,[18] mPW1PW[19] and PBE1PBE[20] (PBE0). The best results were achieved with the mPW1PW functional that provides the lower overestimation of metal-sulfur bond lengths (Table S11), accompanied by a correct evaluation of the NIR absorption wavelength (experimental λ_{max} recorded for **1** in CH_2Cl_2 = 995 nm;[7] calculated in the gas phase 904 nm; calculated in CH_2Cl_2 = 1003 nm). Calculations were extended to complexes **1**–**9**, both as neutral and monoanionic species. An optimization of the wavefunction was carried out to model the singlet diradical description for **1** and **2**. Since a decrease in the agreement between calculated and structural metric parameters and excitation energies were found, the restricted approach was preferred in this work for neutral complexes **1**–**8**, which eventually led to correct bond distances and excitation energies. In addition, the nature of the minima of each optimized structure was verified by harmonic frequency calculations. Only imaginary frequencies related to the combination of the rotations of the four methyl groups (b_{3g}, a_u, b_{2g} and b_{1u}) locked by the D_{2h} symmetry were found. A Natural Population Analysis (NPA) was carried out at the optimized geometries using the Natural Bonding Orbital (NBO) partitioning scheme.[21] Electronic transition

energies and oscillator strength values were calculated at TD-DFT level (10 states). In the case of **1** and **1**$^-$ the independence on the parameters (transition energy, oscillator strength, contribution from monoelectronic excitations) calculated for the NIR-active electron transition on the number of excited states considered was verified. Calculations were carried out also in CH_2Cl_2, $CHCl_3$, CH_3CN, THF and DMF, implicitly taken into account by means of the Polarizable Continuum Model in its Integral Equation Formalism variant (IEF-PCM) describing the cavity of the complexes within the reaction field (SCRF) through a set of overlapping spheres.[22] The contribution of atomic orbitals or molecular fragments to KS-MOs were evaluated by using the program GaussSum 3.0 at the optimized geometries.[23] Oscillator strength values calculated at TD-DFT level were used to evaluate the molar extinction coefficient ε of the investigate compounds.[24] Experimental values of the halfbandwidths on an energy scale (eV or cm^{-1}) W can be directly evaluated from the corresponding values w determined in nm from the experimental NIR spectra recorded in CH_2Cl_2:

$$W = k\frac{w}{{\lambda_0}^2 - \frac{1}{4}w^2}$$

where k is a suitable conversion factor ($k = 10^7$ for cm^{-1}, 1240 for eV energy units). The one-photon absorption oscillator strength of each transition $0 \rightarrow n$ is:[25]

$$f_{0n} = \frac{8\pi^2 m_e \nu_{0n} |\mu_{0n}|^2}{3e^2 h}$$

where m_e and e are the mass and the charge of the electron, ν_{0n} is the frequency (s^{-1}) of the transition between the states 0 and n, μ_{0n} is the transition dipole moment and h is Planck's constant. f_{0n} is related to the experimental intensity of each absorption band:

$$f_{0n} = 4.32 \cdot 10^{-9} \int \varepsilon(\varpi) d\varpi$$

where ε is the molar extinction coefficient (M^{-1} cm^{-1}) and ϖ is the frequency (cm^{-1}). By adopting Gaussian curve-shapes for the absorption bands:

$$f_{0n} = 4.32 \cdot 10^{-9} \varepsilon \int e^{-(\Delta\varpi/\theta)^2} d\varpi$$

$$f_{0n} = 4.32 \cdot 10^{-9}\sqrt{\pi}\varepsilon\theta$$

where the width parameter θ is related to W by:

$$\theta = \frac{W}{2\sqrt{\ln(2)}}$$

Therefore the equation:

$$\varepsilon = \frac{2\sqrt{\ln(2)}}{4.32 \cdot 10^{-9}\sqrt{\pi}} \cdot \frac{f_{0n}}{W}$$

allows evaluating the molar extinction coefficient ε for each transition calculated at TD-DFT level. By assuming ε = 75000 M^{-1} cm^{-1} for **1**, the calculated molar extinction coefficients were correspondingly scaled to get ε_{corr} for **2**–**8** and **1**$^-$–**8**$^-$.

Absolute reduction potentials at 298 K for **1**–**8** were evaluated according to the following equation:[26]

$$E_{Abs}^{298K} = \Delta G_{neutral}^{298K} - \Delta G_{anion}^{298K} - \Delta G_e^{\circ} / F$$

where $\Delta G_{neutral}^{298K}$ and ΔG_{anion}^{298K} are the free energy values calculated at 298 K for **1**–**8** and **1**$^-$–**8**$^-$ and $\Delta G_e^{\circ} / F$ represents the potential of the free electron (-0.03766 eV at 298 K).[27] Reduction potentials referred to the F_c^+/F_c couple ($E_{1/2}^{298K}$) in CH_2Cl_2 were obtained by calculating the thermal corrections to free energies of both neutral and monoanionic solvated species and assuming the correlation previously reported for MeCN solutions:[28]

$$E_{1/2}^{298K} = 1.056 E_{Abs}^{298K} - 4.90$$

Finally, $E_{1/2}^{298K}$ were corrected by 0.060V for the difference in formal potentials of the F_c^+/F_c couple in the two different solvents[29] (the absolute reduction potentials of the F_c^+/F_c couple in acetonitrile and dichloromethane is calculated to differ by 0.045 V at mPW1PW/CRENBL level). The programs GaussView 5.0.9,[30] and Molden 5.2[31] were used to investigate the charge distributions and molecular orbital shapes.

Synthesis

1,3-dimethylimidazole-2-thione and 2-selone were prepared as previously described.[32,33] 1,3-diethyl-2-thioxoimidazolidine-4,5-dione was synthesized according to literature methods.[7,34] Lithium diisopropylamine (LDA) solution (0.26 M) was freshly prepared from diisopropylamine (2.0 mL, 14 mmol) and n-BuLi (8.2 mL of a THF solution 1.6 M) in dry THF (40 mL). Complexes **1**–**8** were synthesised according to the following common procedure.

Complexes 1–8: 4.0 mmol of 1,3-dimethylimidazole-2-thione (0.50 g, for complexes **1**, **2**, **5** and **6**) or 2-selone (0.69 g for complexes **3**, **4**, **7** and **8**) were dissolved under nitrogen in 15 mL of freshly distilled THF and cooled to -10°C in a liquid N_2/ethylene glycol bath. LDA (THF solution 0.26 M, 15 mL, 4.0 mmol) was added dropwise and the reaction mixture was left under stirring for 30 minutes. 5.0 mmol of S (0.17 g for complexes **1**–**4**) or Se (0.39 g for complexes **5**–**8**) were added and, after further 30 minutes, 20 mL of the LDA solution (5.2 mmol) were added. After 3h, a second aliquot (7.0 mmol) of elemental chalcogen was added (0.22 and 0.55 g of elemental sulfur and selenium, respectively), followed by 1.9 mmol of the relevant metal salt ($NiCl_2 \cdot 6H_2O$, 0.45 g, in the case of complexes **1**, **3**, **5**, **7**; K_2PtCl_4, 0.79 g, in the case of **2**, **4**, **6**, and **8**) and 3.9 mmol (0.98 g) of Et_4NI. After 24h, the solid was filtered, washed with ethyl ether and dried under vacuum and stored under argon atmosphere [1.22, 1.29, 0.56, 0.83, 1.98, 1.61, 1.88, and 1.53 g for Et_4N(**1**$^-$)/**1**, Et_4N(**2**$^-$)/**2**, Et_4N(**3**$^-$)/**3**, Et_4N(**4**$^-$)/**4**, Et_4N(**5**$^-$)/**5**, Et_4N(**6**$^-$)/**6**, Et_4N(**7**$^-$)/**7**, and Et_4N(**8**$^-$)/**8**, respectively]. Elemental analyses of all synthesized complexes indicated the presence of a mixture of the neutral species and the tetraethyl ammonium salt of the reduced form of the bis(1,2-dichalcogenolene) complex, as evidenced by NIR absorption measurements. FT-IR spectra were collected on the crude products. **1**: 2979w, 1669m(sh), 1612s, 1439m, 1380m, 1301m, 1286m, 1253w, 1180w, 1132m, 1020m, 863w, 622m, 493vw cm^{-1}; **2**: 3019vw, 2978w, 1682s, 1508w, 1461m, 1412m, 1338m, 1261w, 1186m, 1106s, 1021m, 870w, 800m, 639w, 516vw cm^{-1}; **3**: 3006vw, 2978m, 1646s, 1502s. 1440vs, 1411s, 1379w, 1315m, 1186m, 1127m, 1080w, 1026m, 1003vw, 872m, 797m, 638w, 475w cm^{-1}; **4**: 2976vw, 2831w,

1647s, 1441w, 1337vw, 1115m, 1080m, 1029w, 976s, 898w, 782w, 646w, 514w cm^{-1}; **5**: 3000vw, 2978wm, 1632m, 1541s, 1443vs, 1414m, 1315vw, 1186m, 1027w, 1002m, 861m, 780w, 754w, 679w, 633w, 475m cm^{-1}; **6**: 3000vw, 2978w, 1670m, 1541w, 1458vs, 1411s, 1378vw, 1310vw, 1186s, 1032m, 1003m, 795s, 753w, 515w cm^{-1}; **7**: 3000vw, 2978w, 1671vs, 1567m, 1475w, 1411m, 1356m, 1321s, 1183w, 1133w, 999w, 782m, 512w(br) cm^{-1}; **8**: 2973vw, 2927vw, 1667m, 1578w, 1493s(br), 1438vs, 1354m, 1172w, 1122vw, 1000w, 862w, 820vw, 781w, 634w, 476m(br) cm^{-1}. All the m.p.'s were higher than 210 °C.

Complex 9: a suspension of 1,3-diethyl-2-thioxoimidazolidine-4,5-dione (0.50 g, 2.68 mmol), Lawesson's Reagent (1.50 g, 3.7 mmol), and $PtCl_2$ (0.35 g, 1.31 mmol) was refluxed under dry nitrogen atmosphere for 45 minutes. The reaction mixture was concentrated and poured in methyl alcohol (30mL). The solid was filtered and re-crystallized from CH_2Cl_2/CH_3OH solution. Yield 19%. M.p. > 210°C. Elemental analysis, found (calcd.) C 25.98 (26.62), H 3.16 (3.19), N 8.22 (8.87), S 30.03 (30.45) %. FIR spectrum (500–50 cm^{-1}, polythene pellet): 55w, 390w, 428s cm^{-1}. MIR (3200–500 cm^{-1}, KBr pellet): 2971w, 2961vw, 1416m, 1391s, 1376s, 1350s, 1301m, 1287s, 1257s, 1180w, 1105m, 1082m, 978vw, 953w cm^{-1}. NIR λ_{max} (ε) in CH_2Cl_2 solution (C = $2.61 \cdot 10^{-5}$ M): 998 nm ($79.6 \cdot 10^3$ M^{-1} cm^{-1}). CV measurements (dry CH_2Cl_2, supporting electrolyte Bu_4NBF_4 0.05 M; 298 K; scan rate 0.1 V s^{-1}; ref. el. Ag/AgCl 3.5M): $E_{1/2}$ = -0.622 V vs F_c^+/F_c. FT-Raman (500–50 cm^{-1}, KBr pellet, 350 mW, 5000 scans): 374 cm^{-1}. A small amount of **9** (30 mg, 4.75 mmol) was dissolved in a 30 mL of a 1:3 $CH_3CN/CHCl_3$ mixture and heated for 30 minutes in an Aldrich pressure tube at 120 °C. After cooling, single crystals, suitable for the X-ray diffraction analysis, were filtered off, washed with hexane, and dried under vacuum.

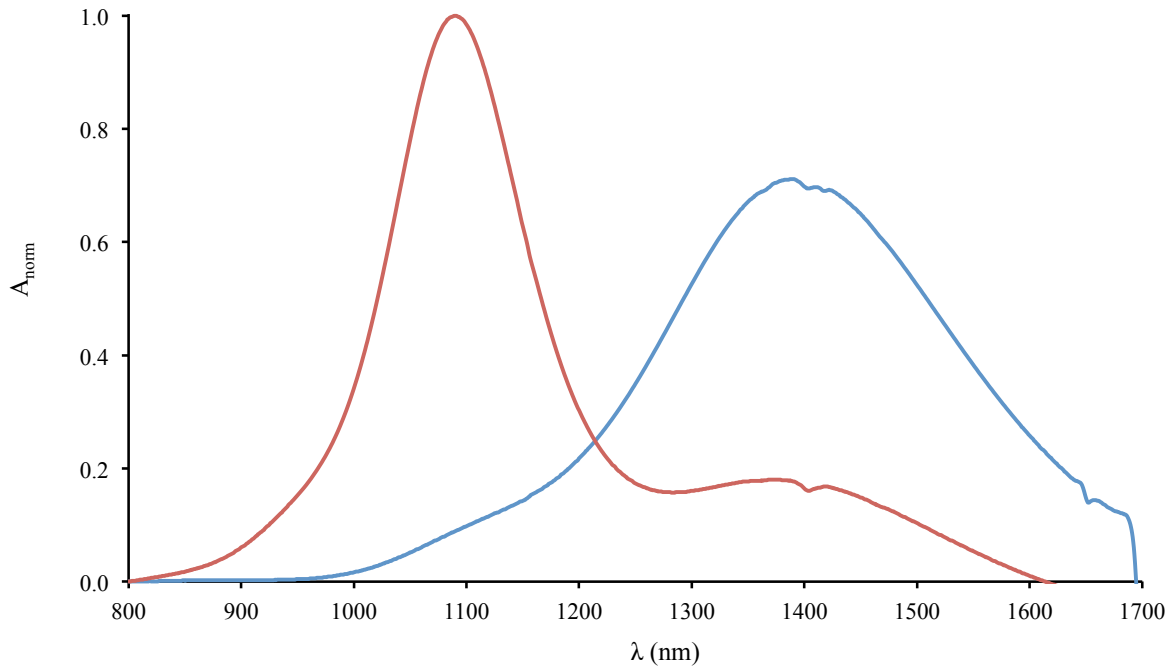

Figure S1. NIR absorption spectra recorded at r.t. for compound $(Et_4N)(\mathbf{5}^-)$ in CH_2Cl_2 solution before (blue; λ_{max} = 1398 nm) and after (red; λ_{max} = 1097 nm) the I_2 oxidation to give **5**. Spectra were normalised to the absorbance of the absorption maximum of the neutral species.

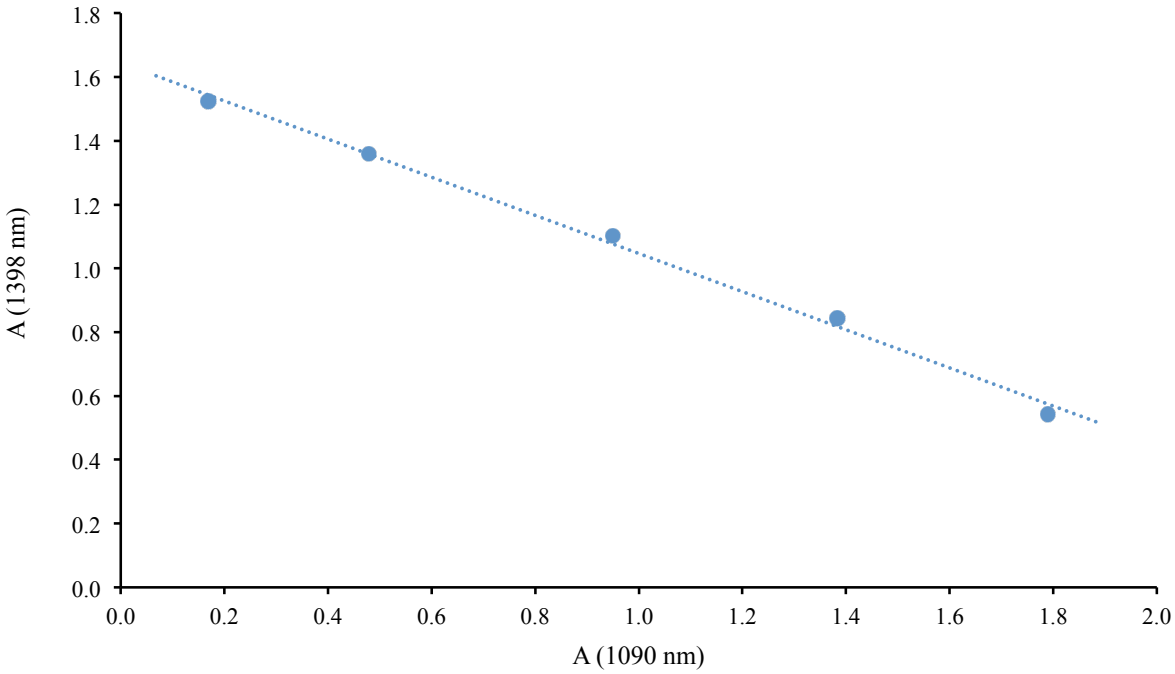

Figure S2. Correlation between the NIR-absorbance A of the band displayed by the monoanion **5**$^-$ (λ_{max} = 1398 nm, Table 1) as a function of the absorbance of the neutral complex **5** (λ_{max} = 1090 nm, Table 1) during the diiodine oxidation in CH_2Cl_2 at r.t. (see Fig. 1). The slope (-0.598) represents the ratio between the molar extinction coefficients of the two differently charged forms. $R^2 = 0.996$.

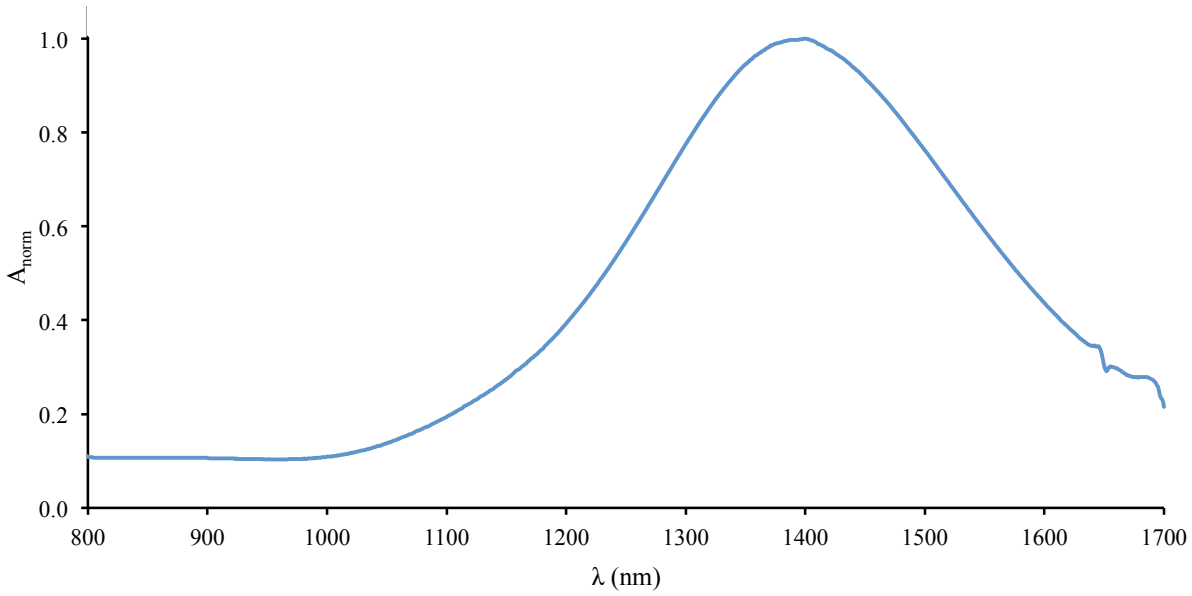

Figure S3. Normalised NIR absorption spectrum of the $(Et_4N)(\mathbf{7}^-)$ in CH_2Cl_2 solution at r.t. (λ_{max} = 1399 nm; Table 1).

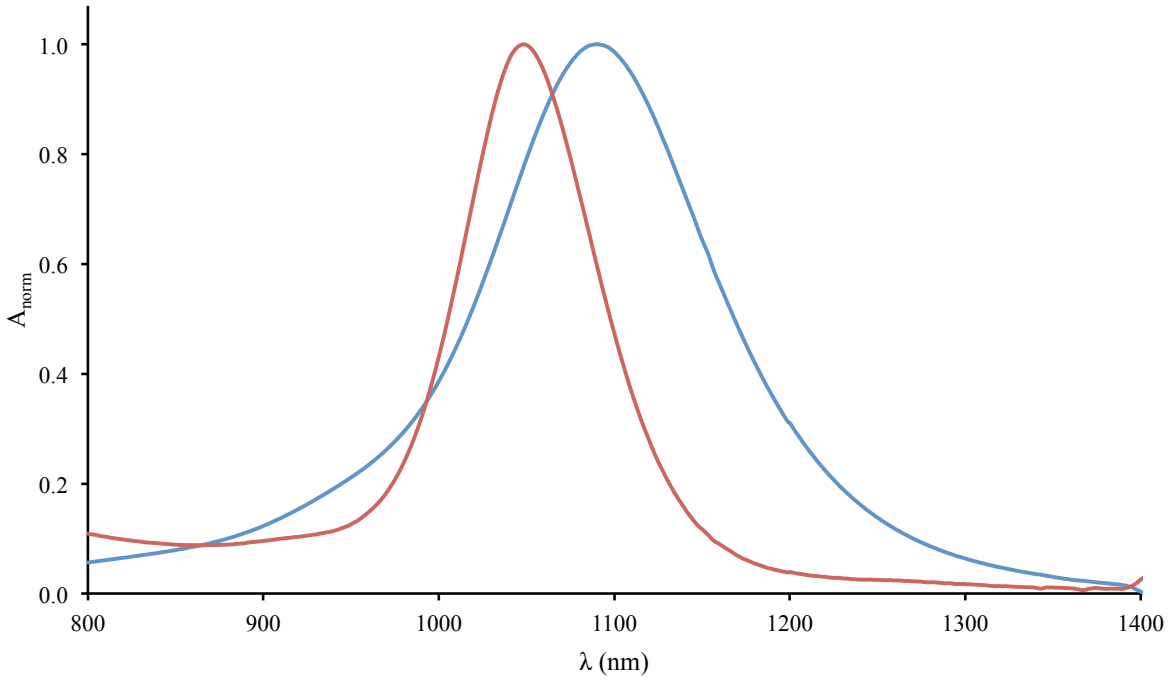

Figure S4. Normalised NIR absorption spectra of the neutral complexes **5** (blue) and **6** (red), differing for the central metal ion (Ni and Pt, respectively), in CH_2Cl_2 solution at r.t. (λ_{max} = 1097 and 1054 nm, respectively; Table 1).

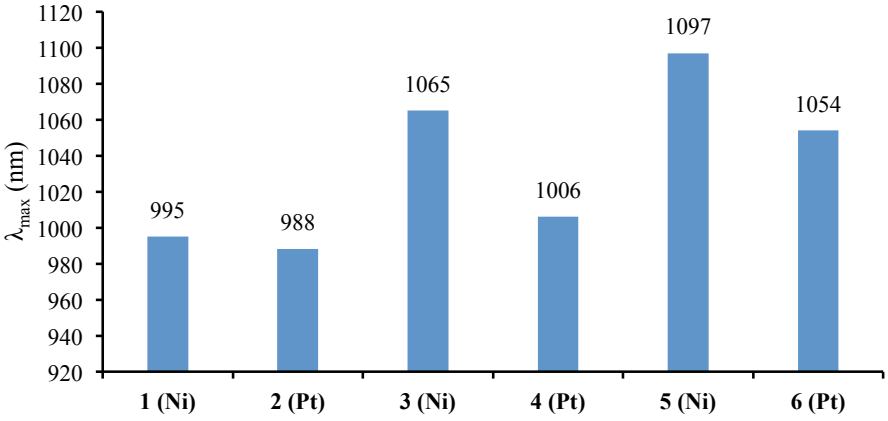

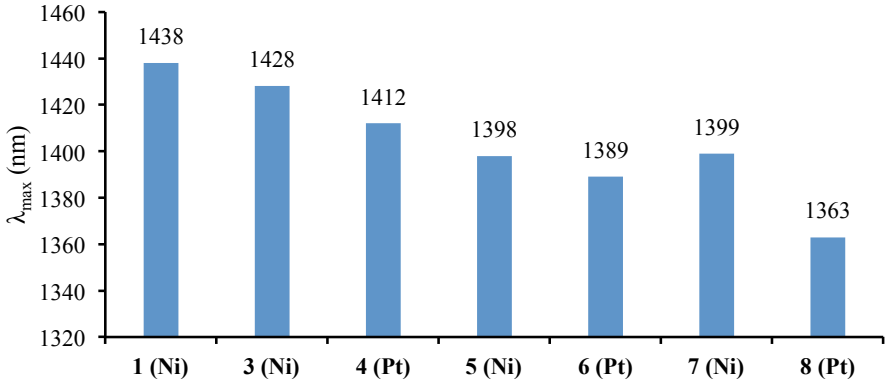

Figure S5. Comparison of the NIR absorption maxima λ_{max} values exhibited by neutral (top) and monoanionic (bottom) bis(1,2-dichalcogenolene) metal complexes reported in Table 1 in CH_2Cl_2 solution at r.t..

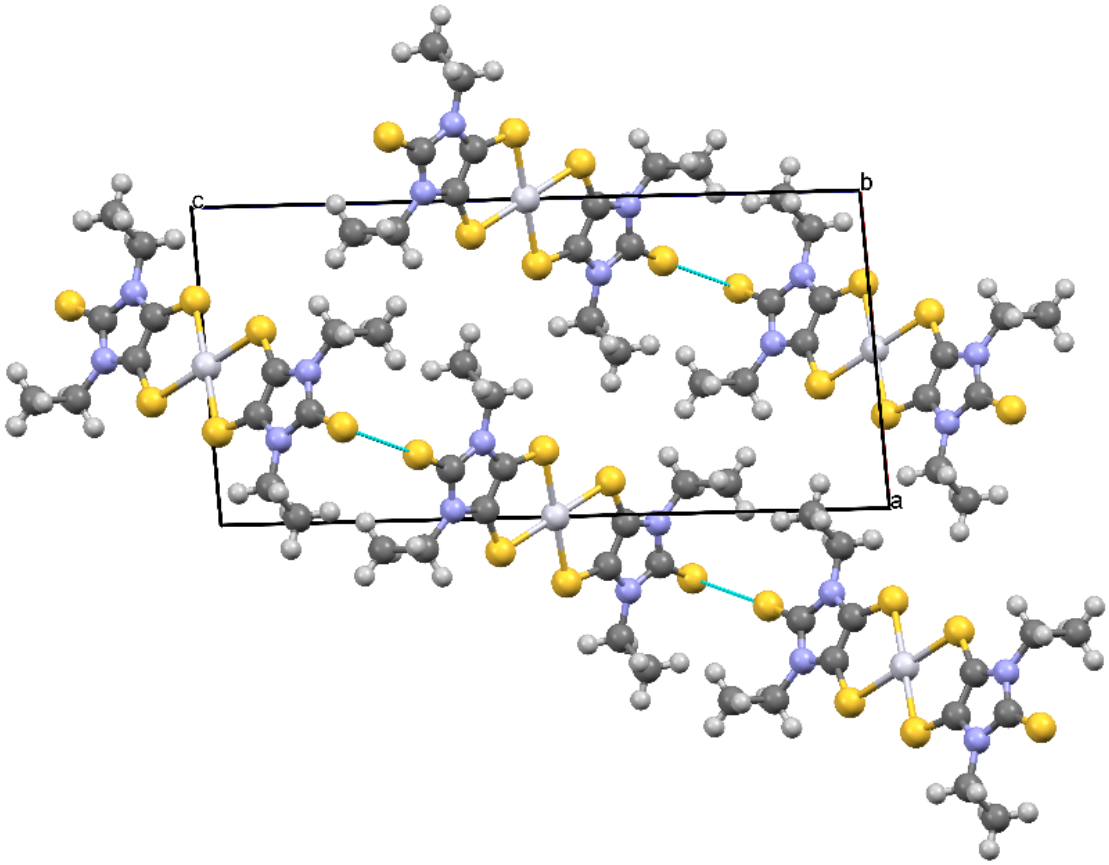

Figure S6. View of the crystal packing of complex **9** view along the *b* axis.

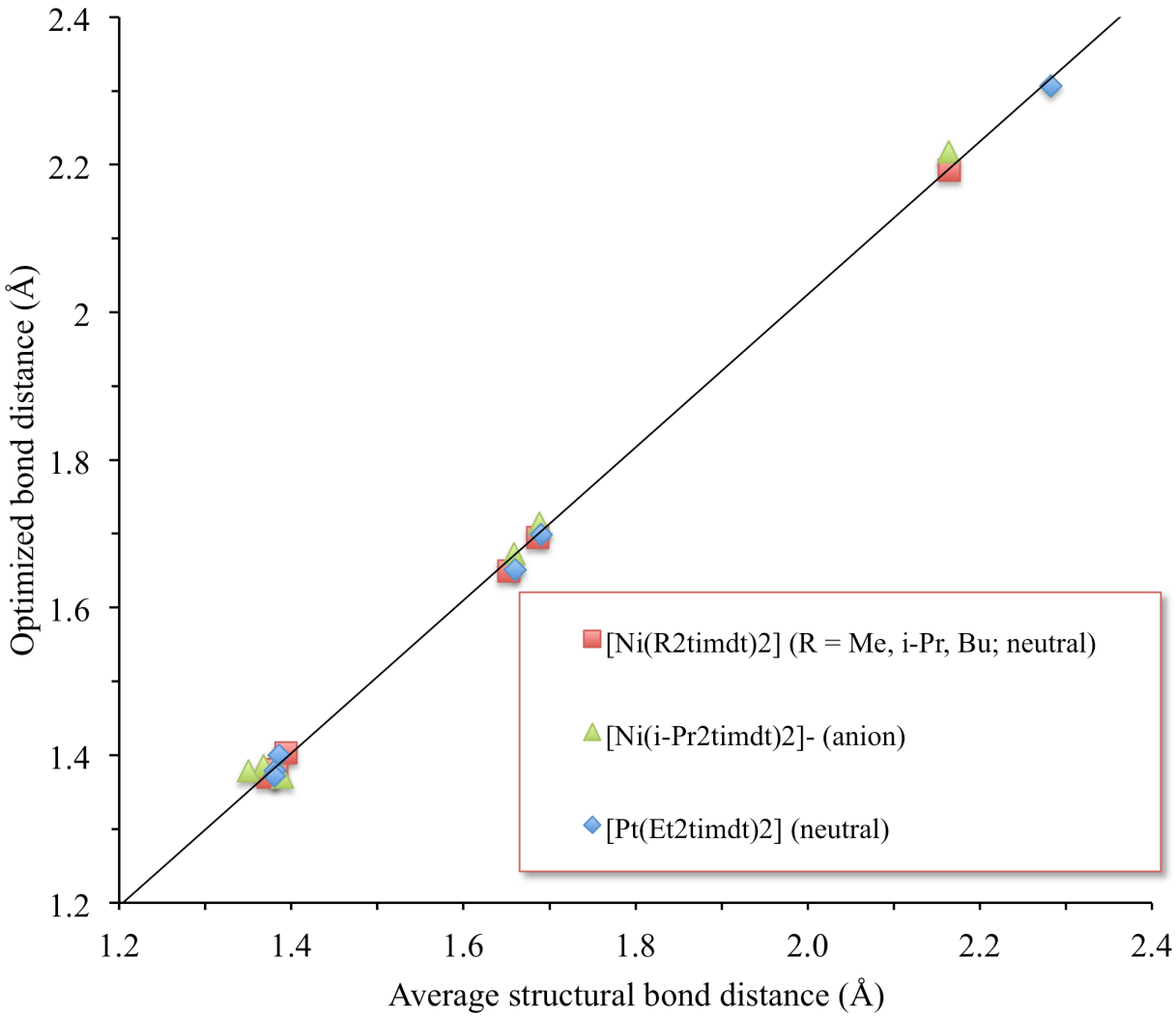

Figure S7. Correlation between C–S, C–N, C–C, and M–S bond distances optimized at DFT level for [Ni(Me_2timdt)$_2$] (**1**), [Ni(Me_2timdt)$_2$]$^-$ (**1**$^-$), and [Pt(Me_2timdt)$_2$] (**9**) and the corresponding average bond lengths determined for [Ni(i-Pr_2timdt)$_2$], [Ni(Bu_2timdt)$_2$], [Ni(Me,i-Pr-timdt)$_2$] (red squares; refs. 6–8), [Ni(i-Pr_2timdt)$_2$]$^-$ (green triangles; ref. 35), and [Pt(Et_2timdt)$_2$] (cyan rhombs, this work). Slope = 1.03; R^2 = 0.998. See Table S11.

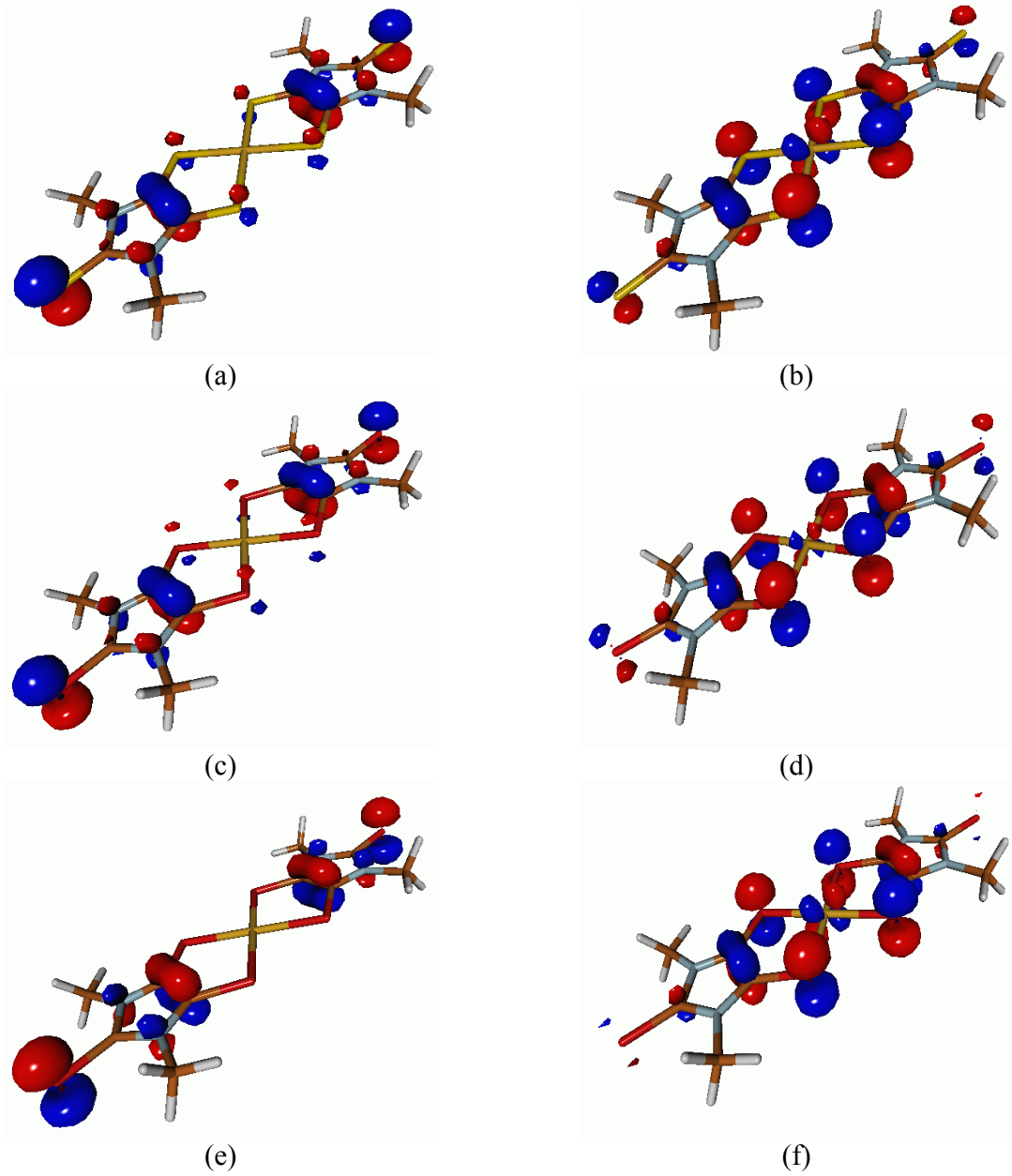

Figure S8. Kohn-Sham HOMOs (left; a, c, and e) and LUMOs (right (b, d, f) calculated for **2** (top; a, b), **7** (middle; c, d), and **8** (bottom; e, f). Cutoff value = 0.05 |e|.

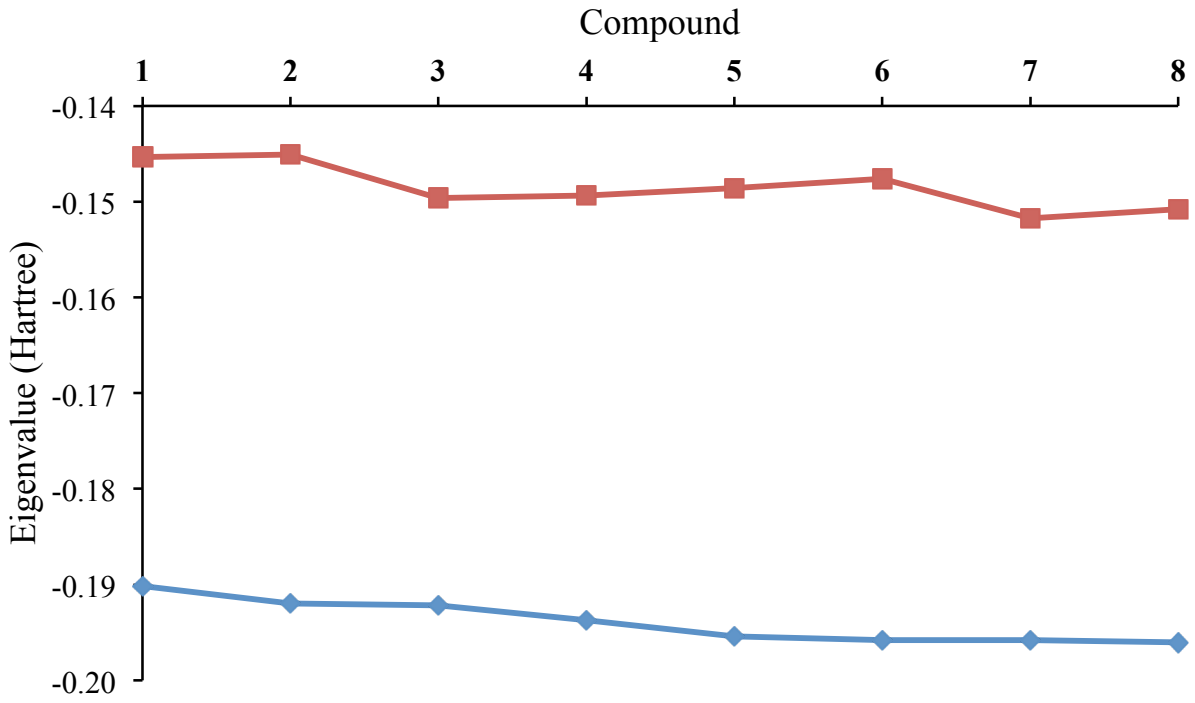

Figure S9. Eigenvalues calculated for KS-HOMOs (blue) and KS-LUMOs (red) in the gas phase for neutral complexes **1**–**8**.

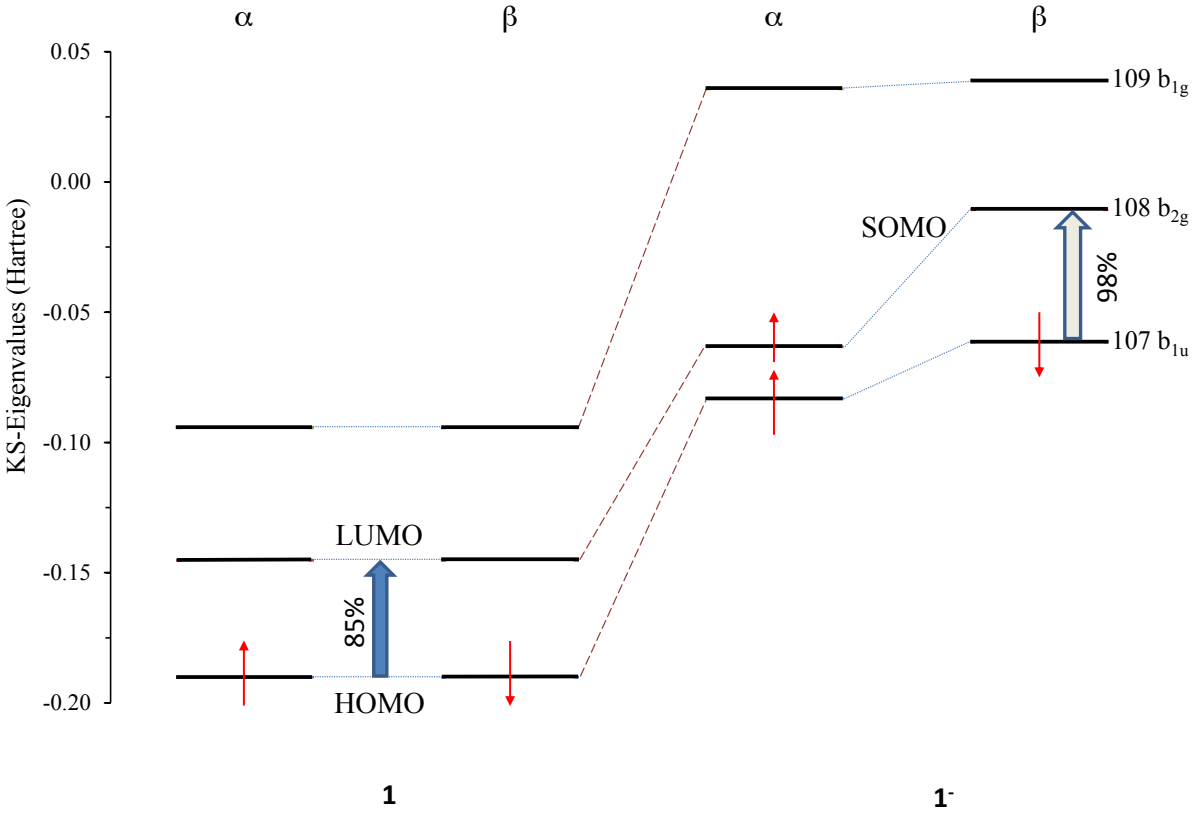

Figure S10. Quantitative MO diagram showing the Kohn-Sham frontier molecular orbitals involved in the NIR transition for **1** and **1**$^{-}$ in the gas phase. According to TD-DFT calculations, the HOMO-LUMO 107b_{1u} → 108 b_{2g} monoelectron excitation accounts for about 85% of the NIR transition of the neutral species **1**, and about 98% for the monoanion **1**$^{-}$.

108-LUMO

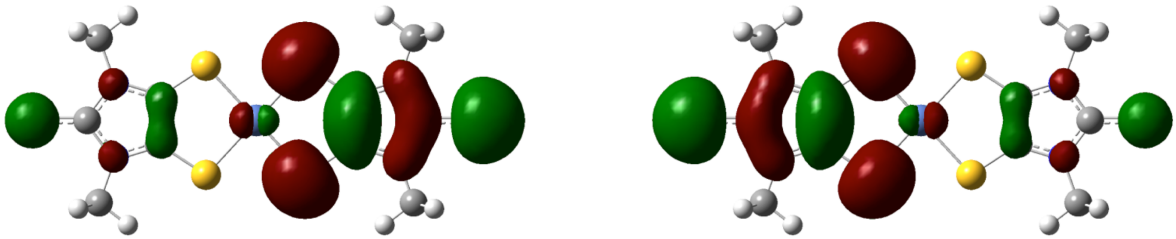

107-HOMO

α-MOs β-MOs

Figure S11. α (left) and β (right) Kohn-Sham HOMO (bottom) and LUMO (top) calculated for **1** in the singlet diradical configuration. Cutoff value = 0.02 |e|.

Table S1. Difference $\Delta\lambda^{0/-1}$ (nm) in the NIR absorption maxima wavelengths exhibited by complexes **1**, **3**, **5**, **6** in their monoanionic and neutral forms in different solvents.

	$\Delta\lambda^{0/-1}$				
	CH_2Cl_2	$CHCl_3$	CH_3CN	THF	DMF
1	443	428	436	442	432
3	363	364	382	365	384
5	301	297	289	359	–
6	335	–	–	324	–

Table S2. NIR absorption maxima wavelengths λ (nm) exhibited by complexes **1**–**8** in their neutral and monoanionic forms in different solvents.

	λ				
	CH_2Cl_2	$CHCl_3$	CH_3CN	THF	DMF
1	995	997	962 [a]	991	998 [a]
1$^-$	1438	1425 [a]	1398	1433	1430
2	988	–	–	–	–
2$^-$	–	–	–	–	–
3	1065	1066	1035 [a]	1074	1051 [a]
3$^-$	1428	1430 [a]	1417	1439	1435
4	1006	–	–	–	–
4$^-$	1412	–	–	–	–
5	1097	1092	1086 [a]	1047 [a]	–
5$^-$	1398	1389 [a]	1375	1406	1402
6	1054	1053	–	1063	–
6$^-$	1389	–	–	1387	1389
7	–	–	–	–	–
7$^-$	1399	1405	1387	1412	1412
8	–	–	–	–	–
8$^-$	1390	1401	1371	1393	1393

[a] Because of solubility reasons, this value was extrapolated with a linear least squares method on the λ values recorded on mixed solvents solutions prepared according to different $V_{solv}/V_{CH_2Cl_2}$ values.

Table S3. Crystal data and details of the structure determination for complex **9**.

Crystal Data			
Formula			C14 H20 N4 Pt S6
Formula Weight			631.79
Crystal System			Monoclinic
Space group		P21/n	(No. 14)
a, b, c [Angstrom]	9.505(3)	5.3533(16)	19.925(6)
alpha, beta, gamma [deg]	90	93.847(9)	90
V [Ang**3]			1011.6(5)
Z			2
D(calc) [g/cm**3]			2.074
Mu(MoKa) [/mm]			7.562
F(000)			612
Crystal Size [mm]		0.01 x	0.01 x 0.30
Data Collection			
Temperature (K)			93
Radiation [Angstrom]		MoKa	0.71073
Theta Min-Max [Deg]			2.0, 25.4
Dataset		-7: 11 ;	-6: 6 ; -20: 23
Tot., Uniq. Data, R(int)		6015,	1820, 0.036
Observed data [I > 2.0 sigma(I)]			1574
Refinement			
Nref, Npar			1820, 116
R, wR2, S		0.0308,	0.0625, 1.06
w = 1/[\s^2^(Fo^2^)+(0.0234P)^2^+2.8618P] where P=(Fo^2^+2Fc^2^)/3			
Max. and Av. Shift/Error			0.00, 0.00
Min. and Max. Resd. Dens. [e/Ang^3]			-1.35, 1.23

Table S4. Final coordinates and equivalent isotropic displacement parameters of the non-hydrogen atoms for complex **9**.

Atom	x	y	z	U(eq) [Ang^2]
Pt1	1	0	1/2	0.0130(1)
S1	0.89290(13)	-0.2229(3)	0.41328(6)	0.0172(4)
S2	1.20747(13)	-0.2117(3)	0.49232(6)	0.0167(4)
S3	1.20369(15)	-0.9580(3)	0.30444(6)	0.0187(4)
N1	1.0276(5)	-0.6035(8)	0.34855(19)	0.0159(12)
N2	1.2380(4)	-0.5975(8)	0.40169(19)	0.0144(12)
C1	1.0259(5)	-0.4164(10)	0.3962(2)	0.0153(17)
C2	1.1590(6)	-0.4121(9)	0.4292(2)	0.0146(17)
C3	1.1562(5)	-0.7197(9)	0.3512(2)	0.0132(16)
C4	0.9085(5)	-0.6673(10)	0.3011(2)	0.0182(17)
C5	0.9081(6)	-0.5045(10)	0.2384(3)	0.0196(19)
C6	1.3851(6)	-0.6542(11)	0.4206(2)	0.0206(17)
C7	1.4839(6)	-0.4857(10)	0.3846(3)	0.0215(19)

U(eq) = 1/3 of the trace of the orthogonalized U Tensor

Table S5. Hydrogen atom positions and isotropic displacement parameters for complex **9**.

Atom	x	y	z	U(iso) [Ang^2]
H4A	0.81910	-0.64340	0.32310	0.0220
H4B	0.91500	-0.84530	0.28820	0.0220
H5A	0.82760	-0.54990	0.20750	0.0300
H5B	0.99590	-0.53040	0.21630	0.0300
H5C	0.90040	-0.32850	0.25120	0.0300
H6A	1.40450	-0.83050	0.40940	0.0250
H6B	1.40290	-0.63320	0.46980	0.0250
H7A	1.58170	-0.52740	0.39880	0.0330
H7B	1.46530	-0.31100	0.39580	0.0330
H7C	1.46830	-0.50970	0.33590	0.0330

The Temperature Factor has the Form of Exp(-T) where

T = 8*(Pi**2)*U*(Sin(Theta)/Lambda)**2 for Isotropic Atoms

Table S6. (An)isotropic displacement parameters for complex **9**.

Atom	U(1,1) or U	U(2,2)	U(3,3)	U(2,3)	U(1,3)	U(1,2)
Pt1	0.0163(2)	0.0109(2)	0.0119(2)	0.0006(1)	0.0007(1)	-0.0003(1)
S1	0.0172(7)	0.0178(7)	0.0164(6)	-0.0015(5)	-0.0012(5)	0.0007(6)
S2	0.0183(7)	0.0160(7)	0.0154(6)	-0.0001(5)	-0.0021(5)	0.0002(5)
S3	0.0210(7)	0.0182(7)	0.0171(7)	-0.0021(5)	0.0022(5)	0.0002(6)
N1	0.020(2)	0.012(2)	0.016(2)	-0.0014(17)	0.0025(17)	-0.0011(19)
N2	0.016(2)	0.010(2)	0.017(2)	0.0038(17)	-0.0005(17)	-0.0015(18)
C1	0.017(3)	0.014(3)	0.015(3)	0.003(2)	0.001(2)	0.002(2)
C2	0.019(3)	0.012(3)	0.013(3)	0.0000(19)	0.0027(19)	-0.001(2)
C3	0.017(3)	0.011(3)	0.012(2)	0.0059(19)	0.0038(19)	-0.001(2)
C4	0.015(3)	0.017(3)	0.022(3	-0.007(2)	-0.003(2)	-0.002(2)
C5	0.018(3)	0.024(4)	0.016(3)	0.001(2)	-0.004(2)	0.000(2)
C6	0.024(3)	0.016(3)	0.021(3)	0.003(2)	-0.004(2)	0.002(2)
C7	0.017(3)	0.029(4)	0.019(3)	0.006(2)	0.004(2)	-0.003(2)

The Temperature Factor has the Form of Exp(-T) Where

T = 8*(Pi**2)*U*(Sin(Theta)/Lambda)**2 for Isotropic Atoms

T = 2*(Pi**2)*Sumij(h(i)*h(j)*U(i,j)*Astar(i)*Astar(j)), for anisotropic Atoms. Astar(i) are Reciprocal Axial Lengths and h(i) are the Reflection Indices.

Table S7. Bond distances (Angstrom) for complex **9**.

Pt1	-S1	2.2825(15)	C1	-C2	1.386(7)
Pt1	-S2	2.2885(15)	C4	-C5	1.523(7)
Pt1	-S1_a	2.2825(15)	C6	-C7	1.517(8)
Pt1	-S2_a	2.2885(15)	C4	-H4A	0.9900
S1	-C1	1.687(5)	C4	-H4B	0.9900
S2	-C2	1.693(5)	C5	-H5A	0.9800
S3	-C3	1.660(5)	C5	-H5B	0.9800
N1	-C1	1.381(6)	C5	-H5C	0.9800
N1	-C3	1.369(7)	C6	-H6A	0.9900
N1	-C4	1.466(6)	C6	-H6B	0.9900
N2	-C2	1.380(6)	C7	-H7A	0.9800
N2	-C3	1.393(6)	C7	-H7B	0.9800
N2	-C6	1.455(7)	C7	-H7C	0.9800

See Table S11 for symmetry code to equivalent positions.

Table S8. Bond angles (Degrees) for complex **9**.

S1	-Pt1	-S2	91.89(5)	N2	-C6	-C7	111.6(4)
S1	-Pt1	-S1_a	180.00	N1	-C4	-H4A	109.00
S1	-Pt1	-S2_a	88.11(5)	N1	-C4	-H4B	109.00
S1_a	-Pt1	-S2	88.11(5)	C5	-C4	-H4A	110.00
S2	-Pt1	-S2_a	180.00	C5	-C4	-H4B	110.00
S1_a	-Pt1	-S2_a	91.89(5)	H4A	-C4	-H4B	108.00
Pt1	-S1	-C1	99.88(16)	C4	-C5	-H5A	109.00
Pt1	-S2	-C2	99.8(2)	C4	-C5	-H5B	109.00
C1	-N1	-C3	110.8(4)	C4	-C5	-H5C	109.00
C1	-N1	-C4	124.6(4)	H5A	-C5	-H5B	110.00
C3	-N1	-C4	124.6(4)	H5A	-C5	-H5C	109.00
C2	-N2	-C3	109.4(4)	H5B	-C5	-H5C	110.00
C2	-N2	-C6	125.9(4)	N2	-C6	-H6A	109.00
C3	-N2	-C6	124.7(4)	N2	-C6	-H6B	109.00
S1	-C1	-N1	128.9(4)	C7	-C6	-H6A	109.00
S1	-C1	-C2	124.5(4)	C7	-C6	-H6B	109.00
N1	-C1	-C2	106.6(4)	H6A	-C6	-H6B	108.00
S2	-C2	-N2	128.5(4)	C6	-C7	-H7A	109.00
S2	-C2	-C1	123.9(4)	C6	-C7	-H7B	109.00
N2	-C2	-C1	107.7(4)	C6	-C7	-H7C	109.00
S3	-C3	-N1	127.1(4)	H7A	-C7	-H7B	110.00
S3	-C3	-N2	127.4(4)	H7A	-C7	-H7C	109.00
N1	-C3	-N2	105.6(4)	H7B	-C7	-H7C	109.00
N1	-C4	-C5	110.8(4)				

See Table S11 for symmetry code to equivalent positions.

Table S9. Torsion angles (Degrees) for complex **9**.

S2	-Pt1	-S1	-C1	1.67(18)
S2_a	-Pt1	-S1	-C1	-178.33(18)
S1	-Pt1	-S2	-C2	-1.51(17)
S1_a	-Pt1	-S2	-C2	178.49(17)
Pt1	-S1	-C1	-N1	178.9(4)
Pt1	-S1	-C1	-C2	-1.6(4)
Pt1	-S2	-C2	-N2	-178.1(4)
Pt1	-S2	-C2	-C1	1.0(4)
C3	-N1	-C1	-S1	-179.4(4)
C4	-N1	-C1	-S1	1.2(7)
C3	-N1	-C1	-C2	1.0(5)
C4	-N1	-C1	-C2	-178.4(4)
C1	-N1	-C3	-N2	-0.9(5)
C1	-N1	-C4	-C5	86.1(5)
C3	-N1	-C4	-C5	-93.2(6)
C4	-N1	-C3	-S3	-2.1(7)
C4	-N1	-C3	-N2	178.5(4)
C1	-N1	-C3	-S3	178.5(4)
C6	-N2	-C3	-N1	-178.0(4)
C6	-N2	-C2	-C1	178.5(4)
C6	-N2	-C2	-S2	-2.2(7)
C3	-N2	-C2	-C1	0.2(5)
C2	-N2	-C6	-C7	-83.5(5)
C3	-N2	-C2	-S2	179.4(4)
C2	-N2	-C3	-S3	-179.0(4)
C6	-N2	-C3	-S3	2.6(7)
C2	-N2	-C3	-N1	0.5(5)
C3	-N2	-C6	-C7	94.6(6)
S1	-C1	-C2	-S2	0.4(6)
N1	-C1	-C2	-S2	-180.0(3)
N1	-C1	-C2	-N2	-0.7(5)
S1	-C1	-C2	-N2	179.7(3)

See Table S11 for symmetry code to equivalent positions.

Table S10. Contact distances (Angstrom) for complex **9**.

S1	.S2	3.285(2)	C4	.C5_h	3.552(8)
S1	.C2	2.723(6)	C5	.C4_i	3.552(8)
S1	.S2_b	3.722(2)	C1	.H5C	3.0900
S1	.S2_a	3.178(2)	C2	.H7B	3.0800
S2	.S1_a	3.178(2)	C4	.H5A_h	3.0300
S2	.S1	3.285(2)	C5	.H4A_i	3.0900
S2	.C1	2.721(5)	C7	.H6B_c	3.0900
S2	.S1_b	3.722(2)	H4A	.S1	2.9400
S3	.S3_f	3.592(2)	H4A	.C5_h	3.0900
S3	.C1_d	3.555(5)	H4B	.S3	2.8100
S3	.C2_d	3.523(5)	H4B	.H5A_h	2.5600
S3	.S3_e	3.592(2)	H5A	.C4_i	3.0300
S1	.H4A	2.9400	H5A	.H4B_i	2.5600
S2	.H6B	2.9800	H5B	.S3_f	2.9400
S2	.H7A_c	3.1800	H5C	.C1	3.0900
S3	.H6A	2.8200	H6A	.S3	2.8200
S3	.H4B	2.8100	H6B	.S2	2.9800
S3	.H5B_e	2.9400	H6B	.C7_c	3.0900
S3	.H7C_e	3.1600	H6B	.H6B_c	2.5700
N1	.N2	2.199(6)	H7A	.S2_c	3.1800
N2	.N1	2.199(6)	H7B	.C2	3.0800
C1	.S3_g	3.555(5)	H7C	.S3_f	3.1600
C2	.S3_g	3.523(5)			

See Table S11 for symmetry code to equivalent positions.

Table S11. Translation of symmetry code to equivalent positions for complex **9**.

a =[3756.00]	= [3_756]	=2-x,-y,1-z	
b =[3746.00]	= [3_746]	=2-x,-1-y,1-z	
c =[3846.00]	= [3_846]	=3-x,-1-y,1-z	
d =[1545.00]	= [1_545]	=x,-1+y,z	
e =[2745.00]	= [2_745]	=5/2-x,-1/2+y,1/2-z	
f =[2755.00]	= [2_755]	=5/2-x,1/2+y,1/2-z	
g =[1565.00]	= [1_565]	=x,1+y,z	
h =[2645.00]	= [2_645]	=3/2-x,-1/2+y,1/2-z	
i =[2655.00]	= [2_655]	=3/2-x,1/2+y,1/2-z	

Table S11. Structural parameters[a] determined by single crystal X-ray diffraction for [Ni(i-Pr_2timdt)$_2$] (A),[b] [Ni(Me,i-Pr-timdt)$_2$] (B),[c] [Ni(Bu_2timdt)$_2$] (C),[d] [Ni(i-Pr_2timdt)$_2$]$^-$ isolated in (Bu_4N)[Ni(i-Pr_2timdt)$_2$] (D)[e] and [Pt(Et_2timdt)$_2$] (**9**)[f] and corresponding metric parameters optimized in the gas phase for [Ni(Me_2timdt)$_2$] (**1**), [Ni(Me_2timdt)$_2$]$^-$ (**1**$^-$), and complex **9** at DFT level.

		Structural data						Calculated metric parameters		
Compound		A[b]	B[c]	C[d]	Aver. A–C	D[e]	**9**[f]	**1**	**1**$^-$	**9**
M		Ni	Ni	Ni	Ni	Ni	Pt	Ni	Ni	Pt
R		i-Pr	Me, i-Pr	Bu	–	i-Pr	Et	Me	Me	Me
Molecular Charge		0	0	0	0	–1	0	0	-1	0
C3-S3	>C=S	1.65(1)	1.644(5)	1.664(4)	1.653(9)	1.654(10) 1.663(10)	1.660(5)	1.6496	1.673	1.6508
C3-N1 C3-N2	(S)C-N	1.40(1) 1.37(2) 1.40(2) 1.38(1)	1.371(6) 1.394(6)	1.376(4) 1.381(4)	1.38(1)	1.36(1) 1.37(1) 1.37(1) 1.37(1)	1.393(6) 1.369(7)	1.380	1.386	1.379
C1-N1 C2-N2	C(C)-N	1.35(2) 1.37(2) 1.40(2) 1.38(1)	1.357(6) 1.373(5)	1.385(4) 1.374(5)	1.37(1)	1.39(1) 1.37(1) 1.40(1) 1.40(1)	1.380(7) 1.381(6)	1.370	1.370	1.372
C1-C2	C-C	1.38(1) 1.39(1)	1.396(6)	1.401(4)	1.39(2)	1.36(1) 1.34(1)	1.386(7)	1.4027	1.3785	1.3996
C1-S1 C2-S2	C-S	1.70(1) 1.69(1)	1.682(5) 1.681(5)	1.678(4) 1.688(4)	1.687(7)	1.663(10) 1.698(10) 1.692(9) 1.699(9)	1.687(5) 1.693(5)	1.6948	1.7147	1.6991
M-S2	M-S	2.161(4) 2.158(4) 2.159(4) 2.156(4)	2.160(1) 2.166(1)	2.1671 2.1769	2.165(6)	2.165(3) 2.161(3) 2.163(3) 2.166(3)	2.2825(15) 2.2825(15)	2.1928	2.2176	2.3071

[a] Atom labelling scheme as in Fig. 2. [b] Taken from ref. 6. [c] Taken from ref. 7. [d] Take from ref. 8. [e] Taken from ref. 35. [f] This work.

Table S12. NIR absorption maximum wavelength λ_{max} (nm) calculated at TD-DFT level for the neutral complex **1** in the gas phase with the hybrid Becke3LYP, mPW1PW and PBE0 functionals, Ahlrichs pVDZ full-electron basis set for C, H, N, S and various ECP sets for the central metal ion (experimental λ_{max} = 995 nm in CH_2Cl_2).

	LANL08(f)	SBKJC	Stuttgart RSC 1997	CRENBL	LANL2DZ	LANL2TZ
B3LYP	899.78	891.77	899.68	944.20	923.71	900.49
mPW1PW	866.89	858.14	867.37	904.34	899.06	866.57
PBE0	861.49	853.85	863.07	902.39	882.57	861.79

Table S13. Eigenvalues (eV) calculated for the frontier molecular orbitals of complexes **1**–**8** and **1**$^{-}$–**8**$^{-}$ in the gas phase and in different solvents at IEF-PCM DFT level

	Gas Phase		CH_2Cl_2		$CHCl_3$		CH_3CN		THF		DMF	
	HOMO	LUMO	HOMO	LUMO	HOMO	LUMO	HOMO	LUMO	HOMO	LUMO	HOMO	LUMO
1	-5.174	-3.954	-5.251	-4.024	-5.240	-4.016	-5.259	-4.029	-5.249	-4.023	-5.260	-4.029
2	-5.224	-3.949	-5.310	-4.019	-5.294	-4.008	-5.324	-4.028	-5.306	-4.016	-5.325	-4.028
3	-5.228	-4.072	-5.317	-4.134	-5.304	-4.129	-5.326	-4.135	-5.314	-4.133	-5.327	-4.135
4	-5.271	-4.064	-5.369	-4.123	-5.351	-4.115	-5.385	-4.128	-5.365	-4.121	-5.385	-4.128
5	-5.317	-4.044	-5.393	-4.107	-5.380	-4.099	-5.404	-4.113	-5.390	-4.105	-5.404	-4.113
6	-5.327	-4.017	-5.408	-4.075	-5.390	-4.063	-5.425	-4.086	-5.403	-4.072	-5.425	-4.086
7	-5.328	-4.129	-5.422	-4.192	-5.406	-4.186	-5.435	-4.196	-5.418	-4.191	-5.435	-4.196
8	-5.334	-4.102	-5.434	-4.156	-5.413	-4.147	-5.454	-4.164	-5.429	-4.154	-5.454	-4.164
	SOMO	LUMO	SOMO	LUMO	SOMO	LUMO	SOMO	LUMO	SOMO	LUMO	SOMO	LUMO
1^{-}	-1.672	-0.292	-4.293	-2.955	-3.984	-2.638	-4.558	-3.226	-4.223	-2.883	-4.561	-3.230
2^{-}	-1.799	-0.272	-4.409	-2.944	-4.096	-2.618	-4.678	-3.228	-4.337	-2.869	-4.681	-3.232
3^{-}	-1.846	-0.492	-4.421	-3.088	-4.118	-2.782	-4.679	-3.349	-4.352	-3.018	-4.683	-3.352
4^{-}	-1.967	-0.462	-4.530	-3.064	-4.225	-2.749	-4.793	-3.336	-4.461	-2.992	-4.797	-3.340
5^{-}	-1.958	-0.494	-4.521	-3.108	-4.217	-2.795	-4.781	-3.378	-4.452	-3.037	-4.785	-3.381
6^{-}	-2.031	-0.450	-4.583	-3.065	-4.275	-2.743	-4.848	-3.346	-4.512	-2.991	-4.852	-3.350
7^{-}	-2.086	-0.659	-4.611	-3.214	-4.313	-2.910	-4.866	-3.474	-4.543	-3.145	-4.870	-3.478
8^{-}	-2.156	-0.611	-4.668	-3.163	-4.367	-2.852	-4.928	-3.434	-4.599	-3.092	-4.931	-3.437

Table S14. Contributions (%) from the metal (M), the ligands, the donor chalcogen atoms X, the terminal chalcogen atoms Y and the C1 atoms of the 1,2-chalcogenolene system to the Kohn-Sham frontier molecular orbitals involved in the NIR transition for complexes **1**–**8** and **1**$^{-}$–**8**$^{-}$.

	Ligand	M[a]	C1[b]	Y[a]	X[a]	Ligand	M[a]	C1[b]	Y[a]	X[a]
			HOMO					LUMO		
1	50	0	8	14	6	48	4	6	8	11
2	49	2	8	15	6	46	8	6	7	12
3	50	0	7	19	6	48	4	6	9	11
4	49	1	7	20	5	46	8	5	8	12
5	50	0	7	15	6	48	5	6	7	12
6	49	1	7	16	6	46	8	5	6	13
7	50	0	6	20	5	48	5	5	9	12
8	49	1	6	21	5	46	8	5	8	13
			HOMO					SOMO		
1^{-}	50	0	8	11	8	47	6	6	5	13
2^{-}	49	2	8	12	8	44	12	5	4	14
3^{-}	50	0	7	14	8	47	6	5	6	13
4^{-}	49	2	7	15	7	44	12	5	5	14
5^{-}	50	0	8	12	8	46	7	5	5	14
6^{-}	49	2	8	12	8	44	12	4	4	15
7^{-}	50	0	7	16	8	46	8	5	5	14
8^{-}	49	2	7	16	7	44	12	4	4	15

[a] X, Y, and M as in Scheme 1. [b] C1 refers to the carbon atoms of the C_2X_2 1,2-dichalcogenolene donor (Fig. 2).

Table S15. Selected bond lengths optimized for complexes **1**–**8** and **1**$^{-}$–**8**$^{-}$ at DFT level.[a,b]

	1	**2**	**3**	**4**	**5**	**6**	**7**	**8**
M-X	2.193	2.307	2.194	2.308	2.298	2.410	2.299	2.411
C(1,2)-X(1,2)	1.695	1.699	1.695	1.700	1.837	1.842	1.838	1.843
C(1)-C(2)	1.403	1.400	1.402	1.399	1.399	1.396	1.399	1.395
C(3)-Y(3)	1.650	1.651	1.806	1.807	1.651	1.652	1.802	1.804
	1^{-}	**2**$^{-}$	**3**$^{-}$	**4**$^{-}$	**5**$^{-}$	**6**$^{-}$	**7**$^{-}$	**8**$^{-}$
M-X	2.218	2.323	2.218	2.328	2.324	2.431	2.323	2.431
C(1,2)-X(1,2)	1.715	1.719	1.714	1.719	1.858	1.862	1.858	1.862
C(1)-C(2)	1.378	1.377	1.379	1.378	1.376	1.375	1.377	1.375
C(3)-Y(3)	1.673	1.673	1.831	1.831	1.672	1.673	1.826	1.827

[a] X, Y, and M as in Scheme 1. [b] Atom labelling Scheme as in Fig. 2.

Table S16. Summary of the NIR electronic transitions calculated at TD-DFT level in the gas phase and at IEF-PCM DFT level in different solvents for complexes **1**–**8** and **1**$^-$–**8**$^-$. For each transition, the most important monoelectronic excitations, their contribution (%) to the NIR transition, the oscillator strength *f*, the energy *E* (eV) and the corresponding calculated wavelength maxima λ (nm) are listed.

		Gas Phase				CH_2Cl_2				$CHCl_3$				CH_3CN				THF				DMF			
	Excit.	%	*f*	*E*	λ	%	*f*	*E*	λ	%	*f*	*E*	λ	%	*f*	*E*	λ	%	*f*	*E*	λ	%	*f*	*E*	λ
1	107-108	84.6	0.487	1.37	904	88.8	0.628	1.24	1003	88.9	0.633	1.23	1008	88.5	0.608	1.26	984	88.7	0.623	1.24	999	88.9	0.629	1.24	1002
1$^-$	107-108	97.7	0.228	0.93	1332	99.0	0.295	0.80	1541	100.0	0.296	0.80	1543	98.8	0.288	0.82	1517	99.0	0.293	0.81	1532	99.0	0.297	0.80	1550
2	107-108	87.7	0.523	1.39	892	90.6	0.666	1.26	985	90.6	0.671	1.25	992	90.2	0.646	1.28	967	90.4	0.661	1.26	982	90.6	0.668	1.26	984
2$^-$	107-108	98.6	0.239	1.02	1220	100.0	0.307	0.89	1396	100.0	0.309	0.89	1398	100.0	0.299	0.89	1394	100.0	0.305	0.89	1396	100.0	0.309	0.87	1420
3	125-126	84.3	0.546	1.32	936	89.0	0.707	1.19	1040	89.0	0.713	1.18	1049	88.6	0.684	1.22	1018	88.8	0.702	1.20	1037	89.1	0.708	1.19	1038
3$^-$	125-126	97.7	0.252	0.92	1348	100.0	0.325	0.80	1544	100.0	0.327	0.80	1550	98.9	0.316	0.82	1515	100.0	0.323	0.81	1536	100.0	0.327	0.80	1549
4	125-126	87.3	0.586	1.34	927	90.8	0.747	1.21	1024	90.8	0.752	1.20	1033	90.5	0.725	1.24	1000	90.7	0.742	1.21	1021	91.0	0.748	1.22	1017
4$^-$	125-126	98.7	0.263	1.01	1227	100.0	0.337	0.89	1396	100.0	0.339	0.89	1394	100.0	0.328	0.90	1381	100.0	0.335	0.89	1388	100.0	0.339	0.88	1407
5	143-144	86.9	0.500	1.38	900	91.3	0.653	1.25	992	91.3	0.659	1.24	998	91.0	0.630	1.27	975	91.2	0.648	1.25	990	91.4	0.654	1.25	992
5$^-$	143-144	98.7	0.228	0.98	1268	100.0	0.304	0.85	1451	100.0	0.304	0.86	1449	100.0	0.295	0.86	1434	100.0	0.301	0.86	1444	100.0	0.306	0.85	1462
6	143-144	89.7	0.519	1.38	900	92.4	0.668	1.26	988	92.4	0.674	1.25	995	92.2	0.647	1.28	970	92.3	0.663	1.26	985	92.5	0.670	1.26	986
6$^-$	143-144	100.0	0.229	1.05	1183	100.0	0.305	0.92	1344	100.0	0.306	0.93	1337	100.0	0.297	0.93	1338	100.0	0.302	0.93	1337	100.0	0.308	0.91	1360
7	161-162	86.5	0.563	1.32	936	91.2	0.737	1.20	1037	91.2	0.743	1.19	1045	91.0	0.711	1.22	1014	91.1	0.731	1.20	1033	91.4	0.738	1.20	1033
7$^-$	161-162	98.6	0.253	0.96	1290	100.0	0.335	0.85	1464	100.0	0.337	0.85	1466	100.0	0.326	0.86	1443	100.0	0.332	0.85	1457	100.0	0.337	0.84	1471
8	161-162	89.2	0.581	1.32	940	92.5	0.748	1.20	1032	92.5	0.754	1.19	1042	92.3	0.724	1.23	1009	92.4	0.743	1.21	1029	92.7	0.749	1.21	1028
8$^-$	161-162	100.0	0.254	1.03	1200	100.0	0.335	0.92	1348	100.0	0.336	0.92	1345	100.0	0.326	0.93	1338	100.0	0.332	0.92	1342	100.0	0.337	0.91	1360

Table S17. Oscillator strength f, energy E (eV), calculated wavelength maxima λ (nm), experimental halfbandwidth expressed in nm (w) and cm^{-1} (W), calculated molar extinction coefficient ε_{calc} ($1000 \cdot M^{-1}$ cm^{-1}) and scaled[a] molar extinction coefficient ε_{corr} ($1000 \cdot M^{-1}$ cm^{-1}) for the NIR electronic transitions calculated at IEF-PCM TD-DFT level in CH_2Cl_2 for complexes **1**–**8** and **1**$^-$–**8**$^-$.

	f	E	λ	w (nm)	W	ε_{calc}	ε_{corr}
1	0.628	1.24	1003	118	1177	116.0	75.0
1$^-$	0.295	0.80	1541	338	1441	44.5	28.8
2	0.666	1.26	985	100	1033	140.1	90.6
2$^-$	0.307	0.89	1396	– [b]	– [b]	– [b]	– [b]
3	0.707	1.19	1040	138	1281	120.0	77.5
3$^-$	0.325	0.80	1544	350	1487	47.5	30.7
4	0.747	1.21	1024	132	1264	128.5	83.1
4$^-$	0.337	0.89	1396	242	1251	58.6	37.9
5	0.653	1.25	992	152	1554	91.4	59.1
5$^-$	0.304	0.85	1451	328	1578	41.9	27.1
6	0.668	1.26	988	90	924	157.2	101.6
6$^-$	0.305	0.92	1344	190	1057	62.7	40.6
7	0.737	1.20	1037	– [c]	– [c]	– [c]	– [c]
7$^-$	0.335	0.85	1464	362	1715	42.5	27.5
8	0.748	1.20	1032	– [c]	– [c]	– [c]	– [c]
8$^-$	0.335	0.92	1348	280	1558	46.7	30.2

[a] Scaled based on the experimental ε value determined for **1**. [b] The absorption band of the monoanion was not found in the NIR spectrum of the reaction product. [c] Diiodine oxidation did not succeed in generating the relevant neutral species.

Table S18. Free energy values ΔG (Hartree) at 298K in CH_2Cl_2 at IEF-PCM-DFT level, absolute (E_{Abs}^{298K}, eV) and relative ($E_{1/2}^{298K}$, V vs F_c^+/F_c) and scaled relative $E_{1/2}^{298K}{}_{\text{corr}}$ reduction potentials calculated for the couples (**1**/**1**$^-$)–(**8**/**8**$^-$) at IEF-PCM-DFT level.

	$\Delta G_{neutral}^{298K}$	ΔG_{anion}^{298K}	$\Delta G_{neutral}^{298K} - \Delta G_{anion}^{298K}$	E_{Abs}^{298K}	$E_{1/2}^{298K}$	$E_{1/2}^{298K}{}_{\text{corr.}}$[a]
1/**1**$^-$	-3164.854	-3165.013	0.1590	4.291	-0.37	-0.31
2/**2**$^-$	-3114.965	-3115.119	0.1534	4.138	-0.53	-0.47
3/**3**$^-$	-7171.542	-7171.702	0.1596	4.306	-0.35	-0.29
4/**4**$^-$	-7121.646	-7121.808	0.1620	4.373	-0.28	-0.22
5/**5**$^-$	-11178.297	-11178.459	0.1628	4.394	-0.26	-0.20
6/**6**$^-$	-11128.418	-11128.573	0.1550	4.181	-0.49	-0.43
7/**7**$^-$	-15185.013	-15185.180	0.1667	4.500	-0.15	-0.09
8/**8**$^-$	-15135.130	-15135.295	0.1649	4.451	-0.20	-0.14

[a] Corrected for the difference in the formal reduction potential of the couple F_c^+/F_c in MeCN and CH_2Cl_2.

References

[1] A. L Fuller, L. A. S. Scott-Hayward, Y. Li, M. Bühl, A. M. Z. Slawin, J. D. Woollins, *J. Am. Chem. Soc.* **2010,** *132* , 5799–5802.

[2] G. M. Sheldricks, *SHELXL-97*, University of Göttingen, Germany, **1997**.

[3] G. M. Sheldrick, *Acta Cryst*. **2008**, *A64*, 112–122.

[4] W. Koch, M. C. Holthausen, in *A Chemist's Guide to Density Functional Theory*, 2nd ed., Wiley-VCH, Weinheim, **2002**.

[5] Gaussian 09, Rev. D.01, M. J. Frisch, G. W. Trucks, H. B. Schlegel, G. E. Scuseria, M. A. Robb, J. R. Cheeseman, G. Scalmani, V. Barone, B. Mennucci, G. A. Petersson, H. Nakatsuji, M. Caricato, X. Li, H. P. Hratchian, A. F. Izmaylov, J. Bloino, G. Zheng, J. L. Sonnenberg, M. Hada, M. Ehara, K. Toyota, R. Fukuda, J. Hasegawa, M. Ishida, T. Nakajima, Y. Honda, O. Kitao, H. Nakai, T. Vreven, J. A. Montgomery Jr., J. E. Peralta, F. Ogliaro, M. Bearpark, J. J. Heyd, E. Brothers, K. N. Kudin, V. N. Staroverov, R. Kobayashi, J. Normand, K. Raghavachari, A. Rendell, J. C. Burant, S. S. Iyengar, J. Tomasi, M. Cossi, N. Rega, J. M. Millam, M. Klene, J. E. Knox, J. B. Cross, V. Bakken, C. Adamo, J. Jaramillo, R. Gomperts, R. E. Stratmann, O. Yazyev, A. J. Austin, R. Cammi, C. Pomelli, J. W. Ochterski, R. L. Martin, K. Morokuma, V. G. Zakrzewski, G. A. Voth, P. Salvador, J. J. Dannenberg, S. Dapprich, A. D. Daniels, O. Farkas, J. B. Foresman, J. V. Ortiz, J. Cioslowski, D. J. Fox, Gaussian, Inc., Wallingford CT, **2009**.

[6] F. Bigoli, P. Deplano, F. A. Devillanova, V. Lippolis, P. J. Lukes, M. L. Mercuri, M. A. Pellinghelli, E. F. Trogu, *J. Chem. Soc., Chem. Commun.* **1995**, 371–372.

[7] M. C. Aragoni, M. Arca, F. Demartin, F. A. Devillanova, A. Garau, F. Isaia, F. Lelj, V. Lippolis, G. Verani, *J. Am. Chem. Soc.* **1999**, 121, 7098–7107.

[8] K. Mebrouk, F. Camerel, O. Jeannin, B. Heinrich, B. Donnio, M. Fourmigué, *Inorg. Chem*. **2016**, *55*, 1296–1303.

[9] A. Schäfer, H. Horn, R. Ahlrichs, *J. Chem. Phys.* **1992**, *97*, 2571–2577.

[10] L. E. Roy, P. J. Hay, R. L. Martin, J. Chem. Theor. Comp. **2008**, *4*, 1029-1031.

[11] W. J. Stevens, M. Krauss, H. Basch, P. G. Jasien, *Can. J. Chem.* **1992**, *70*, 612–630.

[12] M. Kaupp, P. V. R. Schleyer, H. Stoll, H. Preuss, *J. Chem. Phys.* **1991**, *94*, 1360–1366.

[13] W. C. Ermler, R. B. Ross, P. A. Christiansen, *Int. J. Quant. Chem.* **1991**, *40*, 829–846.

[14] W. R. Wadt, P. J. Hay, *J. Chem. Phys.*, **1985**, *82*, 270–283; *ibid.* 284–298; *ibid.* 299–310.

[15] T. H. Dunning Jr., P. J. Hay in "*Methods of Electronic Structure, Theory*", Vol. 2, H. F. Schaefer III ed., Plenum Press, **1977**.

[16] J. V. Ortiz, P. J. Hay, R. L. Martin, *J. Am. Chem. Soc.* **1992**, *114*, 2736–2737.

[17] a) D. Feller, *J. Comp. Chem.* **1996**, *17*, 1571–1586; b) K. L. Schuchardt, B. T. Didier, T. Elsethagen, L. Sun, V. Gurumoorthi, J. Chase, J. Li, T. L. Windus, *J. Chem. Inf. Model*. **2007**, *47*, 1045–1052

[18] A. D. Becke, *J. Chem. Phys.* **1993**, *98*, 5648–5652.

[19] C. Adamo, V. Barone, *J. Chem. Phys.* **1998**, *108*, 664–675 .

[20] C. Adamo, V. Barone, *J. Chem. Phys.* **1999**, *110*, 6158–6170.

[21] A. E. Reed, R. B. Weinstock, F. Weinhold, *J. Chem. Phys.* **1985**, *83,* 735–746.

[22] J. Tomasi, B. Mennucci, R. Cammi, *Chem. Rev.* **2005**, *105*, 2999–3094.

[23] N. M. O'Boyle, A. L. Tenderholt, K. M. Langner. *J. Comp. Chem*. **2008**, *29*, 839–845.

[24] V. Jodaian, M. Mirzaei, M. Arca, M. C. Aragoni, V. Lippolis, E. Tavakoli, N. S. Langeroodi, *Inorg. Chim. Acta* **2013**, *400*, 107–114.

[25] P. N. Day, K. A. Nguyen, R. Pachter, *Chem. Phys. B* **2005**, *109*, 1803–1814.

[26] A. P. Davis, A. J. Fry, *J. Phys. Chem. A* **2010**, *114*, 12299–12304.

[27] J. E. Bartmess, *J. Phys. Chem.* **1994**, *98*, 6420–6424.

[28] V. T. T. Huong, T. B. Tai, M. T. Nguyen, *Phys. Chem. Chem. Phys.* **2016**, *18*, 6259–6267.

[29] N. G. Connelly, W. E. Geiger, *Chem. Rev.* **1996**, *96*, 877–910.

[30] Æ. Frisch, H. P. Hratchian, R. D. Dennington II, T. A. Keith, J. Millam, A. B. Nielsen, A. J. Holder, J. Hiscocks. Gaussian, Inc. GaussView Version 5.0, **2009**.

[31] G. Schaftenaar, J. H. Noordik, *J. Comput.–Aided Mol. Des.* **2000**, *14*, 123–134.

[32] B. L. Benac, E. M. Burgess, A. J. Arduengo III, *J. Org. Synth. Coll.* **1986**, 64, 92–95.

[33] D. J. Williams, M. R. Fawcett-Brown, R. R. Raye, D. VanDerveer, Y. T. Pang, R. L. Jones, K. L. Bergbauer, *Heteroat.Chem*. **1993**, *4*, 409–413.

[34] P. J. Stoffel, *J. Org. Chem*. **1964**, *29*, 2794–2796.

[35] F. Bigoli, P. Deplano, M. L. Mercuri, M. A. Pellinghelli, G. Pintus, E. F. Trogu, G. Zonnedda, H. H. Wang, J. M. Williams, *Inorg. Chim. Acta* **1998**, *273*, 175–183.